



# Fast purification of air from diethyl sulfide with nanosized TiO<sub>2</sub> aerosol

Alexander V. Vorontsov\*, Alexey S. Besov, Valentin N. Parmon

Boriskov Institute of Catalysis and Novosibirsk State University, Novosibirsk 630090, Russian Federation

## ARTICLE INFO

### Article history:

Received 18 June 2012

Received in revised form 7 September 2012

Accepted 13 September 2012

Available online 27 September 2012

### Keywords:

Atmospheric chemistry

CWA

Photocatalysis

Titanium dioxide

Titania

Decontamination

Anti-terrorism

Water concentration

Gas phase

Static

Nanoparticles

Sulfide

Troposphere

## ABSTRACT

TiO<sub>2</sub> aerosol generated by a sonic method has been applied for fast purification of air from diethyl sulfide (DES) vapors inside a closed chamber. Two types of experiments modeling the possible real situations were conducted – (1) aerosol spraying without irradiation followed by UV irradiation after aerosol deposition and (2) aerosol spraying under UV irradiation. Adsorption of DES on TiO<sub>2</sub> particles was complete and fastest at the lowest air relative humidity (RH) while photocatalytic oxidation was fastest at RH 37%. The minimal TiO<sub>2</sub> aerosol surface area needed to remove from air one DES molecule is 2.3 nm<sup>2</sup> at the adsorption and 1.5 nm<sup>2</sup> at the photocatalytic oxidation. The quantum efficiency of the DES consumption increases from 4.7 to 20% when the initial DES concentration increases from 100 to 1000 ppm. The overall quantum efficiency of the DES deep oxidation reached 41 and 58% for the initial concentration 100 and 1000 ppm, respectively. The results demonstrate unusually high activity of TiO<sub>2</sub> aerosol for the adsorption-photocatalytic air purification from DES.

© 2012 Elsevier B.V. All rights reserved.

## 1. Introduction

Development of simple techniques for fast purification of air from hazardous compounds by using compact and mobile equipment is important for avoiding serious consequences of man-caused and natural chemical accidents. A suitable process to perform air purification is adsorption [1]. However, it needs special ventilators or pumps to push air through the adsorbent bed. Contrasting to the fixed bed methods, spraying of fluidized granules or aerosol particles can cover large volumes of contaminated air without sophisticated equipment [2]. In concentrated aerosols of small particles, the characteristic time of air purification can be very short due to small diffusion distances and high mass transfer coefficient to the aerosol particles' for the molecules to be removed from the air [3]. Therefore, duration of air treatment can be very short.

Recently we demonstrated that purification of air from vapors of acetone and dimethyl methylphosphonate (DMMP) using TiO<sub>2</sub> aerosol is performed at the same rate as that of aerosol spraying [4,5]. Adsorption alone on TiO<sub>2</sub> aerosol provides incomplete

air purification from acetone but photocatalytic oxidation on the same aerosol resulted in full air purification. DMMP was completely removed by reactive adsorption over TiO<sub>2</sub> aerosol with characteristic time  $\tau \sim 1$  min, the adsorption being accompanied by the formation of surface hydrolysis product methyl methylphosphonate and release of methanol into air. Photocatalytic oxidation resulted in removal of methanol from the gas phase in less than 10 min.

The aerosol methodology of the emergency air purification has been tested at an example of a surrogate chemical terrorist act using diisopropyl fluorophosphate as chemical agent and mice as a human model [6]. Spraying TiO<sub>2</sub> aerosol cleaned air in about 3 min and thus prevented acute poisoning of mice. However, distant health perspective of animals after their exposure to the concentrated TiO<sub>2</sub> nanoaerosol remained unclear since some nanomaterials are suspected to be toxic. Investigation of such toxic effects is a subject of extensive research. It was found that inhalation of an aerosol of nanosized TiO<sub>2</sub> particles can cause inflammation in mice lungs [7]. Therefore, TiO<sub>2</sub> nanoaerosol should be used with caution for air purification in the presence of humans. The aerosol spraying method has to be considered as useful for very fast discontinuation of exposures to very toxic compounds since the inflammatory aftermath of TiO<sub>2</sub> aerosol can be much better than heavy or lethal health effects of toxic compounds themselves.

\* Corresponding author. Tel.: +7 383 3269447; fax: +7 383 3331617.

E-mail address: [voronts@catalsis.ru](mailto:voronts@catalsis.ru) (A.V. Vorontsov).

A similar technique of air purification was suggested with the application of TiO<sub>2</sub> containing mist produced by ultrasonic irradiation [8]. Aromatic compounds and aldehydes were oxidized photocatalytically in a flow reactor, the partial oxidation products being retained in the aqueous phase of the mist.

Fluidized bed photocatalytic reactors [9,10] also resemble the aerosol approach though relatively large sizes of granules make diffusion distances for the substrate molecules larger than in aerosol [11]. Toluene photooxidation was recently performed on a TiO<sub>2</sub>/SiO<sub>2</sub> composite in the fluidized state, however no advantages of fluidization have been demonstrated [12].

Many organic sulfur compounds possess strong unpleasant odor and increased toxicity. Mustard gas (bis(2-chloroethyl)sulfide) is a blister chemical warfare agent. Photocatalytic destruction of vapors of sulfur compounds proceeds over TiO<sub>2</sub> photocatalyst until complete transformation into inorganic compounds though catalyst deactivation is observed [13]. Such sulfur compounds are interesting object of photocatalysis research since they have low oxidation potentials that guarantees direct oxidation with the photogenerated holes.

The aim of the present work was to determine parameters of adsorption and photocatalytic purification of air from a representative sulfur organic compound, namely diethyl sulfide (DES), using nanosized TiO<sub>2</sub> aerosol. Two regimes of the air purification were studied: with both consecutive and simultaneous adsorption and photocatalytic oxidation at different humidity levels and different initial DES concentrations. It has been found that, in contrast to acetone, DES can be removed from air very quickly by photocatalytic oxidation on TiO<sub>2</sub> aerosol.

## 2. Experimental

### 2.1. Materials

The photocatalyst powder used for the study was TiO<sub>2</sub> Hombifine N (anatase 100%) with specific surface area 300–320 m<sup>2</sup>/g and the primary particles size 5–10 nm [14,15]. Before putting into an aerosol generator, the TiO<sub>2</sub> powder was dried overnight at 120 °C. The low humidity of the powder was important for the efficient aerosol emission. Diethyl sulfide (98%) was purchased from Sigma–Aldrich corporation and used as received.

### 2.2. Reaction setup and methodology

The experimental setup has been described in detail previously [5]. Shortly, it consists from a 100 dm<sup>3</sup> cubic Plexiglas chamber with an aerosol generator placed on its middle bottom, and 22 W annular UV fluorescent mercury lamp TL-E/10 (Philips) at its center. The lamp has emission maximum at 370 nm and the emission line width at half-height 20 nm.

5 g of dried TiO<sub>2</sub> powder was put into the aerosol generator before each experiment. The chamber was then closed and purged with air of the required relative humidity (RH) 4, 37 or 90% through the inlet and outlet ports. The water vapor content in the chamber's air was adjusted to low values by passing air through silica gel. The RH was measured by a humidity meter placed in the flow of air. After the RH of the chamber's air was stabilized, the liquid DES in quantity of 44 or 440 µl was injected into the chamber's injection port with a Hamilton syringe. These amounts of DES correspond to the gas phase concentration of 100 and 1000 ppm, respectively. After the complete evaporation of DES, its concentration slowly decreases due to adsorption and absorption on experimental equipment inside the chamber. This decrease was measured during 1 h and can be taken into account in calculation of air purification rate by aerosol. The TiO<sub>2</sub> powder was aerosolized by 96% during 10 min

of work of the aerosol generator. Thereafter electrical power of the aerosol generator was turned off and the experiment continued with both aerosolized and precipitated TiO<sub>2</sub>. Two types of experiments have been performed. In the first ones, aerosol spraying was performed while the UV lamp was switched off, the UV lamp being turned on after about 2.5 h. In the second type of the experiments, aerosol spraying was done with the UV lamp energized before the start of the spraying.

### 2.3. Analysis

The concentration of gaseous organic compounds, CO and CO<sub>2</sub> in the chamber's air was measured by means of an FT-IR spectrometer Vector-22 (Bruker) equipped with a long path gas cell G-3-8-H (Infrared Analysis Inc.) as described previously [5]. Air from the chamber circulated continuously through the infrared cell with the use of a membrane pump. The following bands were used for the concentration measurements with IR spectroscopy: 2200–2450 cm<sup>-1</sup> for CO<sub>2</sub>, 2750–3100 cm<sup>-1</sup> for DES, 2200–2250 cm<sup>-1</sup> for CO and 2600–2920 cm<sup>-1</sup> or 1650–1900 cm<sup>-1</sup> for acetaldehyde. The spectra were measured from 450 to 4000 cm<sup>-1</sup> with the resolution of 4 cm<sup>-1</sup>. Each spectrum represents an average of 5 scans. The spectra were treated using a software and methodology described in detail in [16].

The primary quantum efficiency of the substrate consumption steps of photocatalytic processes was estimated using the standard formula [17]:

$$\varphi_0 = \frac{W_{N0}}{\Phi}, \quad (1)$$

where  $W_{N0}$  is the rate of the substrate conversion (mol s<sup>-1</sup>) calculated from a concentration–time plot and  $\Phi$  is the incident photon flux (E s<sup>-1</sup>) according to the lamp manufacturer's specification ( $1.2 \times 10^{-5}$  E/s). The overall quantum efficiency of the photocatalytic oxidation into inorganic products was calculated with the equation:

$$\varphi = n \frac{W_N}{\Phi}, \quad (2)$$

where  $W_N$  is the rate of the DES deep oxidation into inorganic products,  $\Phi$  is the incident photon flux,  $n$  is the assumed number of photons needed for the deep oxidation;  $n=32$  for the deep DES oxidation into inorganic products.

## 3. Results and discussion

### 3.1. TiO<sub>2</sub> aerosol generation

Dynamics of the TiO<sub>2</sub> aerosol production by the aerosol generator has been reported previously [5]. The following equation has been suggested there to describe the mass of TiO<sub>2</sub> sprayed,  $m$  (g) as a function of time,  $t$  (min):

$$m(t) = -0.0298t^2 + 0.7728t.$$

However, it was found that in the low spraying time domain, this fit curve deviates from the experimental points. Thus, the simpler function:

$$m(t) = t^{0.69} \quad (3)$$

is suggested and fits the experimental dependence better. We used this function for the treatment of experimental data in obtaining the concentration versus TiO<sub>2</sub> mass curves.

The uniformity of filling the experimental chamber with the TiO<sub>2</sub> aerosol produced can be checked using photographs. Fig. 1 shows the pictures of the chamber at a set of consecutive moments of the TiO<sub>2</sub> aerosol production. One can see the aerosol emission

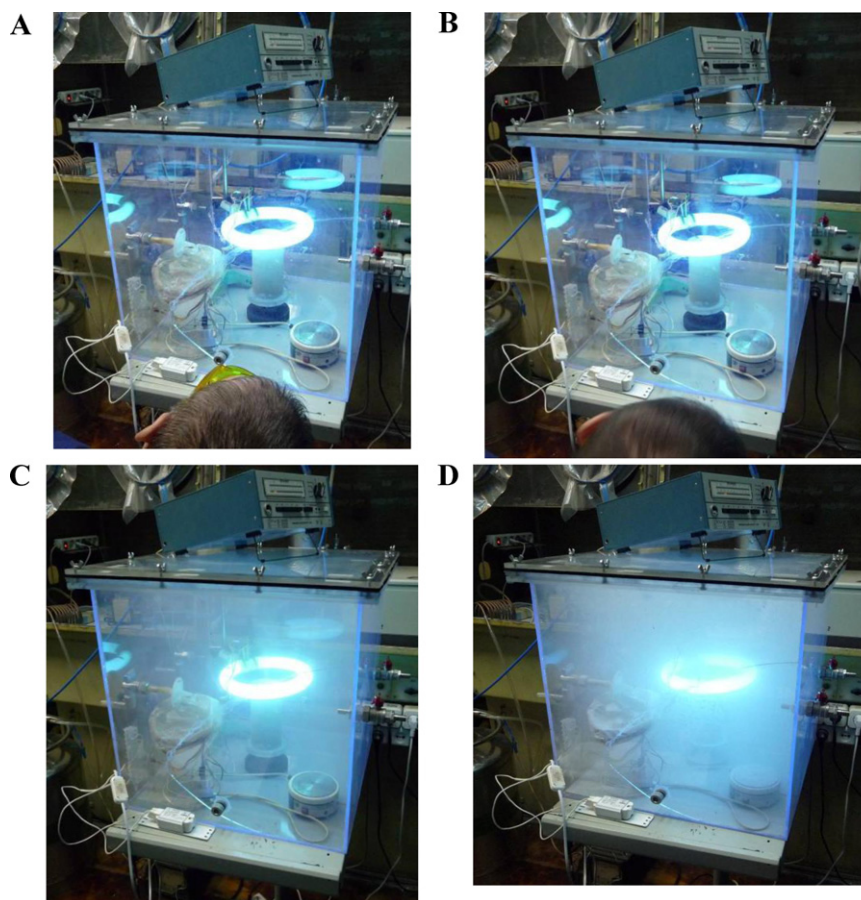


**Fig. 1.** Images of the  $\text{TiO}_2$  aerosol cloud in the chamber at different time after the start of spraying: (A) 0 s, (B) 3 s, (C) 20 s, and (D) 300 s.

from the orifice of the aerosol generator into the chamber's air most clearly in Fig. 1B. At time 20 s (Fig. 1C) the air in the chamber is already quite opaque due to the high concentration of aerosol particles. It seems that the aerosol fills the chamber uniformly due to mixing of air under the action of an air jet created by the aerosol generator. Fig. 1D shows the aerosol at the end of its generation. The visual opaqueness of the aerosol seems to be smaller at the corners of the chamber, which is connected with the smaller thickness of the aerosol layer. Thus, the aerosol produced fills the  $100 \text{ dm}^3$  chamber uniformly which is suitable for the adsorption and photocatalytic experiments.

Two sets of experiments are performed and described below. In the first set of the experiments, the produced  $\text{TiO}_2$  aerosol adsorbed the DES vapor before the UV irradiation started in about 150 min. In the second set of the experiments, the aerosol was sprayed under the UV irradiation so that both adsorption and photocatalytic oxidation proceeded simultaneously.

### 3.2. Consecutive adsorption and photocatalytic oxidation

In the first set of experiments described in this section,  $\text{TiO}_2$  aerosol was used to purify air inside the chamber from DES vapors via two consecutive stages. In the first stage, the UV lamp was off so that the DES removal from the gas phase occurs due to adsorption on  $\text{TiO}_2$  only. After deposition of the aerosol took place, the UV lamp was turned on and the photocatalytic oxidation started. This experiment imitates the air purification procedure with an aerosol cloud during a hypothetical emergency situation. The aerosol is quickly released and, after the air purification, precipitates on the

floor and equipment inside the chamber. Then, the detoxification of the precipitate with the UV radiation was started and resulted in the destruction of the adsorbed organic compounds.

Fig. 2A shows the kinetic curves of the DES removal with the aerosol adsorption and further photocatalytic oxidation at air RH 4%. The experiment started with the DES injection at  $t=0$  min, its evaporation and concentration stabilization. At  $t=72$  min, the aerosol generator was turned on and ran for 10 min. During the aerosol spraying, the DES concentration decreased to practically zero with the characteristic time  $\tau=1.0$  min. Fig. 2B demonstrates the magnified plot of Fig. 2A with the time frame corresponding to the aerosol release period. During 3 min, the DES presence became faint. Thus, fast and complete air purification was attained by adsorption on the  $\text{TiO}_2$  aerosol particles.

Fig. 2A and B shows that after the release of  $\text{TiO}_2$  aerosol, the water vapor concentration decreased by about 1000 ppm and the  $\text{CO}_2$  concentration by 50 ppm because of the adsorption on the  $\text{TiO}_2$  surface. The aerosol precipitated by the time of turning on the UV lamp at  $t=216$  min. Then DES adsorbed on the  $\text{TiO}_2$  particles was gradually oxidized with the release of  $\text{CO}_2$  at the rate of 4.1 ppm/min initially and 1.5 ppm/min in the later part of the experiment. The overall quantum efficiency of the DES oxidation reached 18.5% in the initial period of the oxidation. Water and 5 ppm of CO were also released as products of the photocatalytic oxidation. This experiment showed that at low air humidity, the complete air purification from DES is possible with the adsorption alone. However, the adsorbed DES requires a further treatment.

The experimental dependence of the gas-phase compound concentration on the mass of the adsorbent in the system can be used

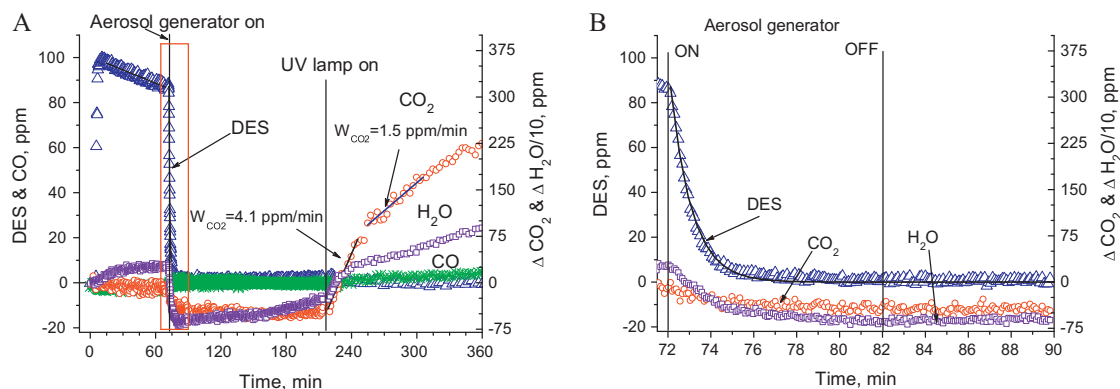


**Fig. 2.** Kinetics of air purification from DES in consecutive adsorption and oxidation at  $C_0(\text{DES}) = 100$  ppm,  $\text{RH} = 4\%$ . (A) Whole time span and (B) time span corresponding to adsorption stage.

to obtain parameters of adsorption isotherm via fitting to the following Langmuir isotherm derived equation [5]:

$$C = 0.5[C_0 - \beta m - \kappa + \sqrt{(\kappa - C_0 + \beta m)^2 + 4\kappa C_0}], \quad (4)$$

where  $C$  is the gas phase concentration (ppm),  $C_0$  is the concentration before the adsorption (ppm),  $\beta = N/\alpha$  (ppm g<sup>-1</sup>),  $\kappa = 1/K$  (ppm),  $N$  is the adsorption site mass density (mol sites g<sup>-1</sup>),  $m(t)$  is the mass of adsorbent as a function of the experiment time  $t$  (g),  $\alpha$  is the dimension transformation coefficient (mol ppm<sup>-1</sup>)  $\alpha = 10^{-6}(\text{PV}/RT) = 4.09 \times 10^{-6}$  at  $T = 298$  K,  $P = 101,325$  Pa,  $V = 0.1$  m<sup>3</sup>,  $R = 8.314$  J K<sup>-1</sup> mol<sup>-1</sup>, and  $K$  is the adsorption constant (ppm<sup>-1</sup>).

The experimental points of DES concentration plotted versus the mass of TiO<sub>2</sub> sprayed are shown in Fig. 3 together with the fit curve according to Eq. (4). The fit of the curve gives the following parameter values:  $N = 2.32 \times 10^{-4}$  mol/g and  $K = 0.49$  ppm<sup>-1</sup>. The corresponding adsorption site area for one DES molecule is 2.3 nm<sup>2</sup>. This method for obtaining the adsorption isotherm parameters has been applied previously for adsorption of acetone on TiO<sub>2</sub>. At the same air humidity of 4%, the acetone adsorption site area was 2.14 nm<sup>2</sup> and the adsorption constant was  $K = 0.0037$  ppm<sup>-1</sup>. It is interesting to notice that the adsorption constant for DES is higher significantly than that for acetone while the adsorption site area is similar. This can be due to the strong interaction of sulfur atom of DES with the titanium surface sites Ti<sub>5</sub>C.

From a practical point of view, such low humidity as 4% is rarely met, the usual values of RH being in the 30–90% range. Purification

of air from the DES vapors at a higher value of air humidity 37% demonstrates a different behavior than that observed for the almost dry air. Fig. 4 demonstrates the kinetic curves for the consecutive adsorption of the DES vapor and photocatalytic oxidation over the precipitated TiO<sub>2</sub> aerosol particles. Aerosol spraying was started at  $t = 65$  min and resulted in only 30% reduction of the DES concentration. The characteristic time of the DES concentration decrease  $\tau = 2.9$  min is larger than that at low humidity. This different behavior is obviously due to the water vapor molecules competition for the surface adsorption sites. This is confirmed by a marked decrease in the water vapor concentration during aerosol spraying by nearly 300 ppm (Fig. 4). After the completion of the aerosol spraying, the DES concentration showed a slow decrease at 0.04 ppm/min due to the slow adsorption on TiO<sub>2</sub> particles and materials of experimental equipment. The water vapor concentration showed some fluctuations.

At  $t = 223$  min, the UV lamp was turned on. This resulted in a fast decrease of the DES vapor concentration. The characteristic time of the DES concentration decrease due to the photocatalytic oxidation is  $\tau = 4.5$  min; the concentration approaches zero in less than 30 min. The initial rate of the DES consumption is  $W_0(\text{DES}) = 8.3$  ppm/min. At the same time, the CO<sub>2</sub> concentration increases with the rate of 3.7 ppm/min and the water vapor concentration increases as well. The rate of the CO<sub>2</sub> production is similar to the case of low humidity (Fig. 2). The overall process of deep

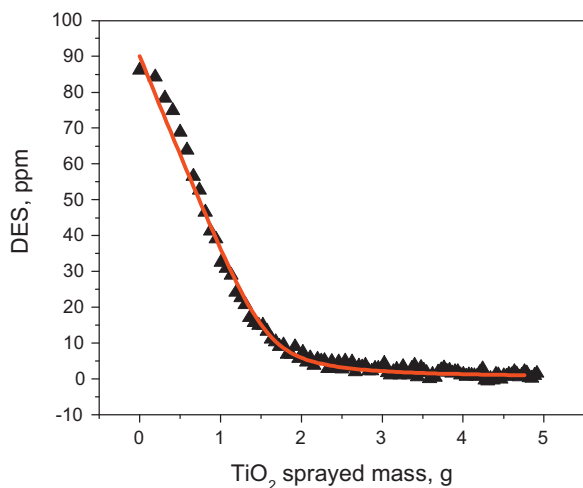


**Fig. 3.** The effect of the mass of TiO<sub>2</sub> sprayed as aerosol on the concentration of gaseous DES in the adsorption experiment shown in Fig. 2B.

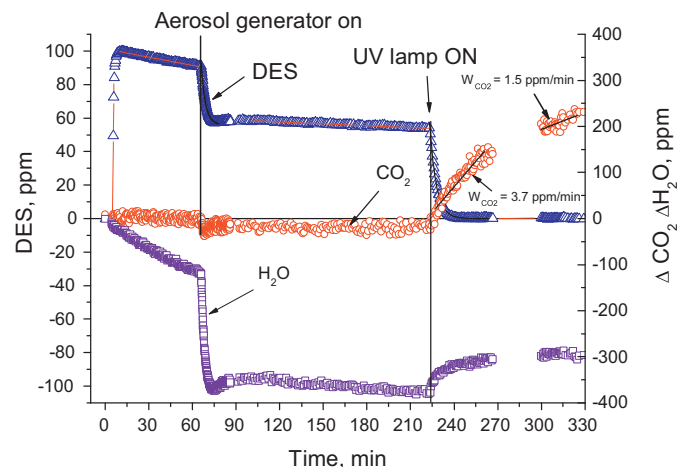


**Fig. 4.** Kinetics of the air purification from DES vapors at the consecutive adsorption and oxidation at  $[\text{DES}]_0 = 100$  ppm,  $\text{RH} = 37\%$ .



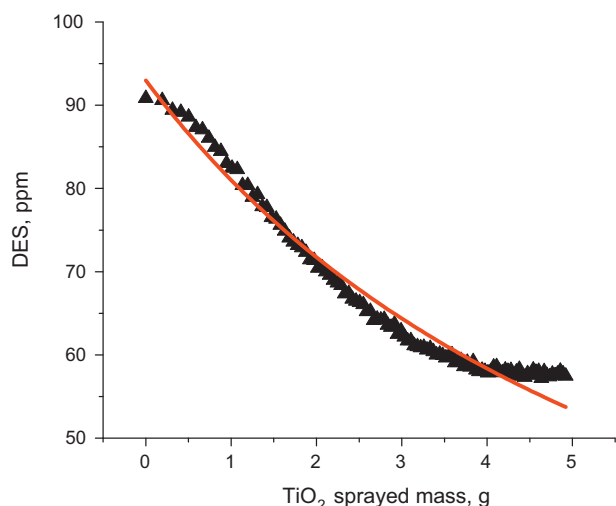
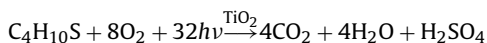


**Fig. 5.** The effect of the mass of  $\text{TiO}_2$  sprayed as aerosol on the concentration of gaseous DES in the adsorption experiment shown in Fig. 4.

photocatalytic oxidation of adsorbed DES is described by equation:



Thus, there is an obvious discrepancy between the DES amount consumed and the  $\text{CO}_2$  and  $\text{H}_2\text{O}$  amount observed experimentally in Fig. 4. The partial oxidation products seem to be accumulated on the  $\text{TiO}_2$  surface because the DES oxidation proceeds much easier than the oxidation of products of its partial oxidation [13]. Assuming that one photon is needed to convert DES molecule into some surface products, Eq. (1) gives quantum efficiency of initial DES consumption  $\varphi_0 = 4.7\%$ . The quantum efficiency of the DES complete oxidation into  $\text{CO}_2$  is calculated with Eq. (2) using the value of the initial rate of the  $\text{CO}_2$  formation and equals to  $\varphi = 17\%$ .

The final products of the DES oxidation process are vapor of water, gaseous carbon dioxide and sulfuric acid residing on the surface of the photocatalyst [18]. The accumulation of sulfuric acid on the photocatalyst surface results in a gradual catalyst deactivation. This can be the reason for the decrease of the carbon dioxide production rate at the later stages of the oxidation. This experiment demonstrates that photocatalytic oxidation is very efficient for air purification from the DES vapors at ambient air humidity. The adsorption alone is inefficient but photocatalytic oxidation of DES proceeds with a high quantum efficiency.

The dependence of the DES concentration on the mass of  $\text{TiO}_2$  sprayed as aerosol during the adsorption phase for the experiment at RH 37% is represented in Fig. 5. Eq. (3) was utilized to fit the experimental points, the curve corresponding to the fitting results. One can see that the curve describes satisfactorily the experimental data with some deviations possibly due to irregularities in the aerosol spraying. The adsorption isotherm parameters obtained are  $N = 2.32 \times 10^{-4} \text{ mol/g}$  and  $K = 3.0 \times 10^{-3} \text{ ppm}^{-1}$ . The corresponding adsorption site area is same as for the experiment at low RH. The effective adsorption constant decreased by two orders of magnitude since it takes into account the competition of the water vapor. Obviously, a larger amount of the  $\text{TiO}_2$  aerosol is required for the adsorptive air purification at RH 37%.

### 3.3. Simultaneous adsorption and photocatalytic oxidation

The process of destruction of DES and air purification could be accelerated if both processes, adsorption and photocatalytic oxidation, proceed at the same time. The combined procedure results are

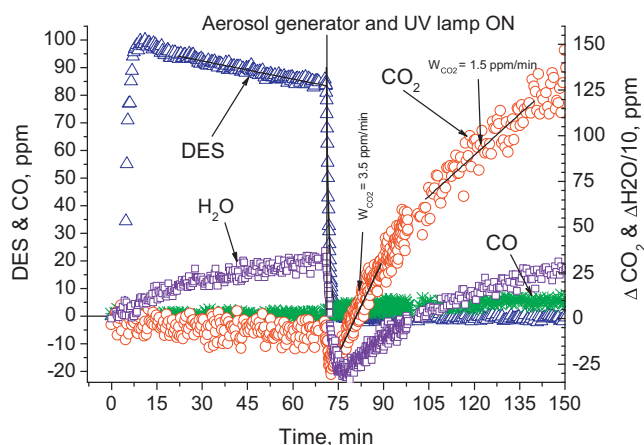


**Fig. 6.** Kinetics of the air purification from DES vapors at the simultaneous adsorption and photocatalytic oxidation at  $[\text{DES}]_0 = 100 \text{ ppm}$ , RH = 4%.

shown in Fig. 6 for air relative humidity 4% and the initial concentration of DES 100 ppm.

Liquid DES was injected into the chamber at  $t = 0 \text{ min}$ , then it evaporated and reached a pseudo steady concentration. At  $t = 70 \text{ min}$ , the aerosol generation started and the UV lamp was switched on. One can see that the DES concentration dropped rapidly down to nearly zero in 3 min. The DES concentration decrease follows the first-order kinetics with characteristic time 0.85 min. This is considerably faster than at the purely adsorptive air purification by the same  $\text{TiO}_2$  aerosol as shown in Fig. 2A and B. Simultaneously with the DES concentration drop, the  $\text{CO}_2$  concentration decreased by ca. 25 ppm and water vapor concentration decreased by ca. 300 ppm due to the adsorption on  $\text{TiO}_2$  particles. Then, one can see that the  $\text{CO}_2$  concentration increased in the course of the DES photocatalytic oxidation. There are two regions of the  $\text{CO}_2$  concentration rise: the first one with the slope of 3.5 ppm/min and the second one with 1.5 ppm/min. Some quantity of CO was also formed in the DES photocatalytic oxidation. Table 1 summarizes some characteristic parameters of the air purification and photocatalytic oxidation. The quantum efficiency of the DES deep oxidation into  $\text{CO}_2$  calculated according to Eq. (2) using the value of the initial rate of  $\text{CO}_2$  formation equals to  $\varphi = 16\%$ .

The adsorption and photocatalytic oxidation of DES is shown in Fig. 7 for air RH 37%. Liquid DES was injected into the chamber at  $t = 0 \text{ min}$ . After the DES evaporation its concentration reached a pseudo steady level, and the UV lamp was turned on at  $t = 30 \text{ min}$ .

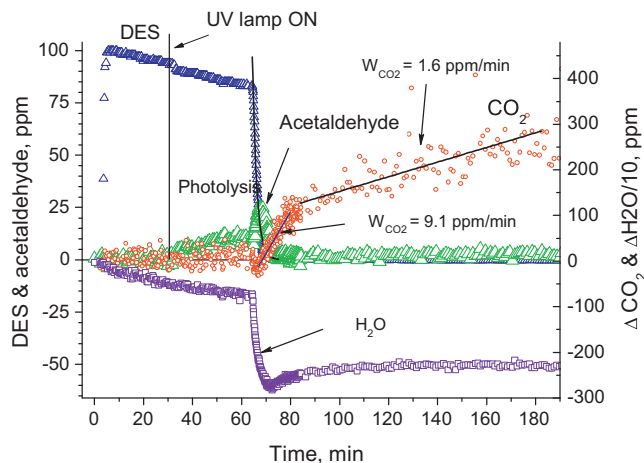


**Fig. 7.** Kinetics of the air purification from DES vapors at the simultaneous adsorption and photocatalytic oxidation at  $[\text{DES}]_0 = 100 \text{ ppm}$ , RH = 37%.

**Table 1**

Parameters of the air purification from DES via the adsorption and photocatalytic oxidation.

$C_0(\text{DES})$ , ppm	$C_f(\text{DES})$ , ppm	Air humidity, %	$\tau_{\text{ads}}$ , min	$\tau_{\text{DES}}$ , min	$W_0(\text{CO}_2)$ , ppm/min	$W_0(\text{C}_2\text{H}_4\text{O})$ , ppm/min
100	~0	4	1.0	–	4.1	–
100	59	$37 \pm 3$	2.9	–	3.7	–
100	~0	4	–	0.85	3.5	–
100	~0	$37 \pm 3$	–	1.8	9.1	4.8
100	~0	$90 \pm 5$	–	4.5	8.25	6.7
1000	~0	$37 \pm 3$	–	47	12.8	7.5

Designations:  $C_0(\text{DES})$ , the initial concentration of DES;  $C_f(\text{DES})$ , the final concentration of DES;  $\tau_{\text{ads}}$ , the characteristic time of the DES removal by adsorption;  $\tau_{\text{DES}}$ , the characteristic time of the DES removal by the adsorption and photocatalytic oxidation;  $W_0(\text{CO}_2)$ , the initial rate of the  $\text{CO}_2$  formation at the DES photocatalytic oxidation;  $W_0(\text{C}_2\text{H}_4\text{O})$ , the initial rate of the acetaldehyde formation at the DES photocatalytic oxidation.

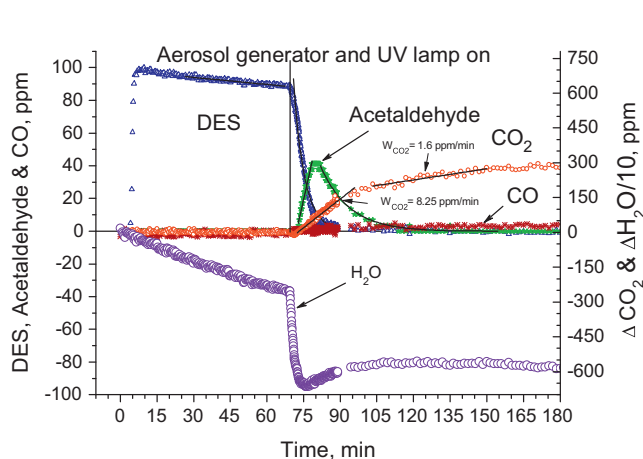
The gas phase was irradiated for 30 min thereafter in order to check the contribution of the direct DES photolysis. One can see that the rate of the DES concentration decrease changed as a result of photolysis from  $0.16 \pm 0.01$  ppm/min to  $0.27 \pm 0.01$  ppm/min. The formation of acetaldehyde was also observed at the rate of  $0.23 \pm 0.02$  ppm/min. However, the carbon dioxide and water vapor concentrations were not affected by the DES photolysis thus indicating that the photolysis results in slow partial oxidation only. The overall concentration of DES in the chamber has not changed during the photolysis significantly. At  $t = 60$  min, the aerosol generator was turned on. This led to a dramatically fast decrease of the DES concentration and the rise in the  $\text{CO}_2$  concentration with the rate of 9.1 ppm/min. After 30 min of the photocatalytic oxidation, the  $\text{CO}_2$  production rate decreased to 1.6 ppm/min. The overall quantum efficiency of the DES oxidation into  $\text{CO}_2$  was  $\varphi = 41\%$  at the start of the oxidation. This is markedly higher compared to the lower humidity case as Table 1 demonstrates and is higher than the rate of photocatalytic oxidation of acetone and dimethyl methylphosphonate at the same conditions [5]. The positive effect of the increase in RH on the photocatalytic oxidation in the aerosol system has already been reported in [5] for dimethyl methylphosphonate. Therefore it was interesting to prove whether a higher RH would be beneficial for the adsorptive-photocatalytic air purification from DES.

Fig. 8 demonstrates the dynamics of the gas phase concentrations during purification of air from DES at initial RH 90%. At  $t = 0$  min, liquid DES was injected into the chamber and evaporated. After equilibration of the gas phase composition, the aerosol generator and the UV lamp were turned on at  $t = 70$  min. One can see that the DES concentration decreases slower than at lower RH. The characteristic time of the DES removal is 4.5 min which is at least twice longer than that at lower RH. The concentration of DES decreases by 90% during the aerosol spraying period ( $t = 70$ –80 min). Also,

the formation of acetaldehyde is observed and its concentration reaches its maximum of nearly 40 ppm at  $t = 80$  min.  $\text{CO}_2$  is generated at the rate of 8.3 ppm/min initially, however this rate decreases later to the steady value of 1.6 ppm/min. Thus, the steady rate of the  $\text{CO}_2$  generation is not affected by the experimental conditions. The overall quantum efficiency of the DES oxidation for the initial oxidation period comprises  $\varphi = 37\%$ . So, one can conclude that the increase of RH to 90% negatively influences the performance of the aerosol method of air purification. One can assume that this is associated with the competition of water vapor for the DES adsorption sites. Fig. 8 shows that the water vapor concentration decreases by only about 5000 ppm just after the aerosol spraying; thus, according to the BET isotherm, the  $\text{TiO}_2$  surface is covered with several layers of water molecules during the photocatalytic oxidation, and the thickness of water is higher at RH 90% than at RH 37%. This affects strongly the dynamics of DES adsorption since non-polar DES molecules should penetrate thicker layer of water. The rate of partial and complete DES oxidation is affected moderately (see Table 1) because the surface is covered with water layers in the both cases and only its concentration increases.

The results reported above were obtained with the DES quantity of  $44 \mu\text{l}$  (0.41 mmol). It was found that more than 90% of this quantity was removed from the gas phase either by adsorption alone or by adsorption and photooxidation in less than 10 min at any humidity levels. The DES molecules surface density for the  $\text{TiO}_2$  used comprises  $0.15 \text{ nm}^{-2}$  or  $6.5 \text{ nm}^2$  per one DES molecule which is a large surface area. Therefore it was interesting to determine the capacity of  $\text{TiO}_2$  aerosol for air purification by injecting larger quantity of DES.

Fig. 9 shows results of the adsorptive-photocatalytic removal of DES injected in quantity of 4.1 mmol into the experimental chamber. After equilibration of the gas phase, the aerosol generator and



**Fig. 8.** Kinetics of the air purification from DES vapors at the simultaneous adsorption and photocatalytic oxidation at  $[\text{DES}]_0 = 100$  ppm, RH = 90%.

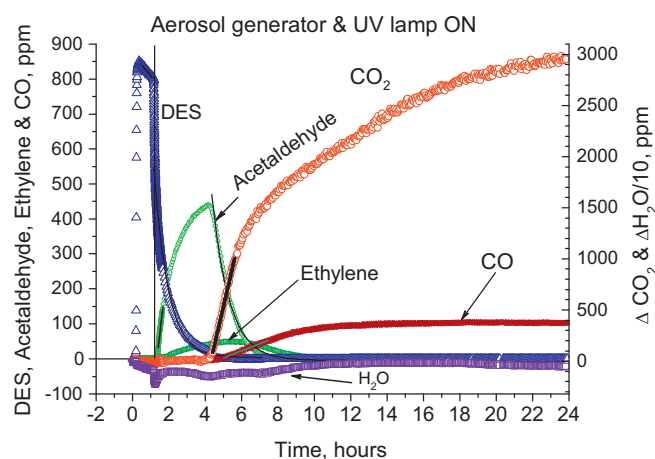


**Fig. 9.** Kinetics of the air purification from DES vapors at the simultaneous adsorption and photocatalytic oxidation at  $[\text{DES}]_0 = 1000$  ppm, RH = 37%.

the UV lamp were switched on at  $t = 70$  min. During the aerosol spraying time (70–80 min), the DES concentration decreased from 796 to 433 ppm at the average rate of 36 ppm/min. The rate corresponds to the initial quantum efficiency of the DES consumption  $\varphi_0 = 20\%$ . Thus, 5 g of  $\text{TiO}_2$  is capable of consuming 1.76 mmol DES that corresponds to 0.66 molecules/nm<sup>2</sup>. This confirms the previously obtained result on the air purification from dimethyl methylphosphonate (DMMP) that around 1 nm<sup>2</sup> of  $\text{TiO}_2$  surface area is needed to purify air from each DMMP molecule [19].

After completion of  $\text{TiO}_2$  aerosol spraying, further air purification proceeds due to the photocatalytic oxidation only. The formation of a significant amount of intermediate gaseous products is detected such as acetaldehyde, ethylene and CO. The later product is not consumed even after 23 h of oxidation possibly due to the deactivation of the photocatalyst surface by such products.  $\text{CO}_2$  starts to be produced only when almost all gaseous DES is consumed and the acetaldehyde concentration reaches its maximum. The rate of the  $\text{CO}_2$  production is first 12.8 ppm/min which corresponds to the overall quantum efficiency of the DES oxidation  $\varphi = 58\%$ . This is a high value close to that for the other organic molecules oxidation at their high concentration. Later, the rate of the  $\text{CO}_2$  generation decreases due to the catalyst deactivation and exhausting the intermediates to be oxidized. After one day of the oxidation, all organic compounds are oxidized into inorganic products. The formation of CO in the concentration of about 100 ppm is the result of catalyst overloading with the initial substrate and its oxidation products.

#### 4. Conclusions

Vapors of diethyl sulfide (DES) can be fast removed from air via adsorption and photocatalytic oxidation over  $\text{TiO}_2$  nanosized aerosol particles. It is possible to perform the air purification in either consecutive or simultaneous adsorption and photooxidation. The following peculiarities were observed:

- the air purification from DES is fastest at the simultaneous adsorption-photocatalytic mode;
- the rise of the air relative humidity (RH) from 4 to 37% affects negatively the DES adsorption but increases the rate of its photocatalytic oxidation. Excessive humidity of 90% somewhat decreases the photooxidation rate as well;

- the highest overall quantum efficiency of the DES oxidation at RH 37% was  $\varphi = 41\%$  at the initial DES concentration 100 ppm and  $\varphi = 58\%$  at the initial DES concentration 1000 ppm;
- the  $\text{TiO}_2$  surface area taken to purify air from one DES molecule is about 2.3 nm<sup>2</sup> for the purely adsorption process and 1.5 nm<sup>2</sup> for the photocatalytic oxidation on aerosol particles.

#### Acknowledgements

We gratefully acknowledge the support of ISTC (project 3305), the Ministry of Education and Science of Russia (contract 16.513.11.3091, federal target program “Scientific and educational personnel”), Presidium RAS grant 24.49 and Russian Federation President grant for the Leading Scientific Schools NSH-524.2012.3.

#### References

- [1] R.M.A. Roque-Malherbe, Adsorption and Diffusion in Nanoporous Materials, CRC Press, 2007.
- [2] EPA APTI Training Course 415: Control of Gaseous Emissions, Adsorption, 2008 (Chapter 4).
- [3] H. Blum, H.C. Siegmann, *Surface Science* 603 (2009) 1969–1978.
- [4] A.S. Besov, A.V. Vorontsov, *Catalysis Communications* 9 (2008) 2598–2600.
- [5] A.S. Besov, A.V. Vorontsov, V.N. Parmon, *Applied Catalysis B: Environmental* 89 (2009) 602–612.
- [6] A.S. Besov, N.A. Krivova, A.V. Vorontsov, O.B. Zaeva, D.V. Kozlov, A.B. Vorozhtsov, V.N. Parmon, G.V. Sakovich, V.F. Komarov, P.G. Smirniotis, N. Eisenreich, *Journal of Hazardous Materials* 173 (2010) 40–46.
- [7] V.H. Grassian, A. Adamcakova-Dodd, J.M. Pettibone, P.T. O’Shaughnessy, P.S. Thorne, *Nanotoxicology* 1 (2007) 211–226.
- [8] K. Sekiguchi, D. Noshiroya, M. Handa, K. Yamamoto, K. Sakamoto, N. Namiki, *Chemosphere* 81 (2010) 33–38.
- [9] H.P. Kuo, C.T. Wu, R.C. Hsu, *Powder Technology* 210 (2011) 225–229.
- [10] H. Gao, C. Si, J. Zhou, G. Liu, *Journal of the Taiwan Institute of Chemical Engineers* 42 (2011) 108–113.
- [11] M. Shiraiwa, R.M. Garland, U. Poschl, *Atmospheric Chemistry and Physics* 9 (2009) 9571–9586.
- [12] M. Tasbihi, U.L. Stangar, U. Cernigoj, J. Jirkovsky, S. Bakardjieva, N.N. Tusar, *Catalysis Today* 161 (2011) 181–188.
- [13] A.V. Vorontsov, *Russian Chemical Reviews* 77 (2008) 909–926.
- [14] S.C. Chan, M.A. Barteau, *Topics in Catalysis* 54 (2011) 378–389.
- [15] E.N. Kabachkov, E.N. Kurkin, V.A. Nadtochenko, A.A. Terent’ev, *High Energy Chemistry* 44 (2010) 426–430.
- [16] D. Kozlov, A. Besov, *Applied Spectroscopy* 65 (2011) 918–923.
- [17] S.E. Braslavsky, *Pure and Applied Chemistry* 79 (2007) 293–465.
- [18] A.V. Vorontsov, E.N. Savinov, C. Lion, P.G. Smirniotis, *Applied Catalysis B: Environmental* 44 (2003) 25–40.
- [19] D.A. Trubitsyn, A.V. Vorontsov, *Journal of Physical Chemistry B* 109 (2005) 21884–21892.